

A Dynamical Labelling Method for Extracting Partial Structure Factors

M.ARAI¹, A.C.HANNON² and T.OTOMO³

1) Dept. of Physics, Kobe University, 1-1 Rokkodai, Nada, Kobe 657, Japan

2) ISIS facility, Rutherford Appleton Laboratory, Chilton, Didcot Oxon OX11 0QX, UK

3) Institute for Materials Research, Tohoku University, Katahira, Sendai 980, Japan

This paper discusses a new data analysis scheme for the scattering function $S(Q,E)$ covering a wide range of Q - E space. The dynamic pair correlation function (DPCF) method has been developed to obtain the real space correlation at excitation energy E by analogy with diffraction data analysis. Two typical examples, SiO_2 glass and high- T_C superconductors, have been employed to depict the potential of the DPCF method. For a material which contains significantly different masses the DPCF may provide the partial structure factor for the light atoms.

INTRODUCTION

In recent decades neutron scattering has provided a unique probe for studying the structure and dynamics of materials; both diffraction and spectroscopic techniques may be employed. However, it is only comparatively recently that it was clearly shown experimentally that more detailed and unique information about the structure and the vibrational states can also be obtained from the momentum dependence (Q -dependence) of the scattering function $S(Q,E)$. A specific model calculation may be used to obtain insight into the structure apparent in reciprocal-space, i.e. in the Q -dependence of $S(Q,E)$. However,

an alternative approach was proposed theoretically in 1975 by Carpenter and Pelizzari [1] whereby a real space correlation function is used to interpret the Q -dependence of $S(Q,E)$. The recently developed pulsed spallation neutron source spectrometer, MARI [2], offers an ideal opportunity to explore this idea experimentally for the first time with a very wide Q - E range, cf. Fig.1 [3]. In this report we will discuss how we obtain the dynamic pair correlation function (DPCF) from $S(Q,E)$ by use of an approach developed by analogy with the procedure used for diffraction data. We will show two typical cases, vitreous SiO_2 and the high- T_C superconductor $\text{YBa}_2\text{Cu}_3\text{O}_7$, studied by MARI.

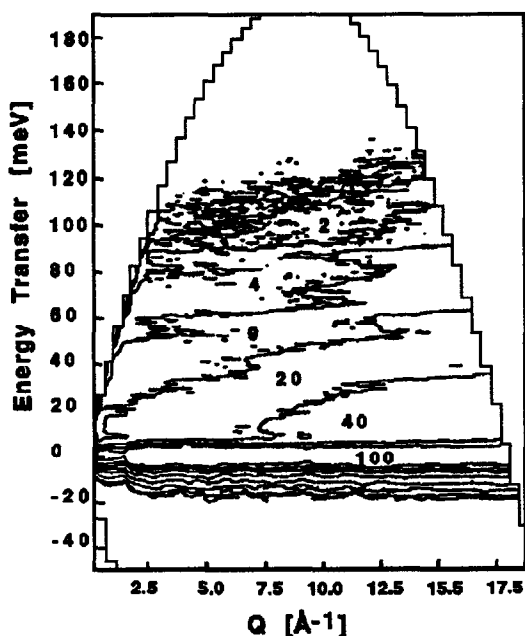


Fig.1 $S(Q,E)$ of $\text{La}_{1.85}\text{Sr}_{0.15}\text{CuO}_4$,
 $E_i=200\text{meV}$

From these examples we will see:

- 1) The DPCF may provide partial structure factor information without isotope substitution when the material contains elements with significantly different masses.
- 2) The DPCF is very sensitive to some local structural instability, which may have been neglected or overlooked in previous neutron scattering studies when using conventional data analysis methods.

DYNAMIC PAIR CORRELATION FUNCTION

The neutron cross section is written as

$$\frac{d^2\sigma}{d\Omega dE} = N \frac{k_1}{k_0} \langle b^2 \rangle S(Q, E). \quad (1)$$

The dynamical structure factor $S(Q, E)$ for one-phonon scattering [4] is

$$S(Q, E) = \frac{1}{N \langle b^2 \rangle} \left[\sum_{i, i'} e^{-i(W_i + W_{i'})} (b_i b_{i'}) \exp(iQ \cdot [i' - i]) \right. \\ \left. \times \sum_j \frac{\hbar^2 (\mathbf{Q} \cdot \mathbf{e}_i^{j*}) (\mathbf{Q} \cdot \mathbf{e}_{i'}^j)}{2\sqrt{M_i M_{i'}} E} \langle n_j(\omega) + 1 \rangle \delta(E - \hbar\omega_j) \right] \langle Q \rangle \quad (2)$$

where $W_i = u_i^2 / 6$ is the Debye-Waller factor and the atomic displacement vector \mathbf{u}_i is expressed using normalised vectors \mathbf{e}_i^j and the quantum harmonic operator a_j

$$\mathbf{u}_i(t) = \sum_j \left(\frac{\hbar}{2M_i \omega_j} \right)^{1/2} \left[\mathbf{e}_i^j \exp(-i\omega_j t) a_j + \mathbf{e}_i^{j*} \exp(i\omega_j t) a_j^+ \right]. \quad (3)$$

If the material under consideration has the long-range order of a crystal, we can apply translational invariance by using $\mathbf{i} = \mathbf{l} + \mathbf{d}$, where \mathbf{l} is a translational vector of the crystal and \mathbf{d} is a vector in the unit cell, cf. Fig.2. Thus,

$$\mathbf{e}_i^j = \frac{1}{N^{1/2}} \sum_q \mathbf{e}_d^j(q) \exp(iq \cdot (\mathbf{l} + \mathbf{d})). \quad (4)$$

The cross-section for a crystal then takes the well-known form

$$S(Q, E) = \frac{1}{N \langle b^2 \rangle} \frac{(2\pi)^3}{v_0} \left[\sum_{d, d'} e^{-i(W_d + W_{d'})} (b_d b_{d'}) \exp(iQ \cdot [d' - d]) \right. \\ \left. \times \sum_{jq} \frac{\hbar^2 (\mathbf{Q} \cdot \mathbf{e}(q)_d^{j*}) (\mathbf{Q} \cdot \mathbf{e}_d^j(q))}{2\sqrt{M_d M_{d'}} E} \langle n_j(\omega) + 1 \rangle \delta(E - \hbar\omega_j(q)) \sum_{\tau} \delta(\mathbf{Q} - \mathbf{q} - \boldsymbol{\tau}) \right] \langle Q \rangle. \quad (5)$$

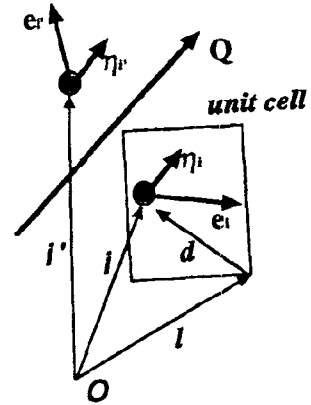


Fig.2 Relation of Vectors.

If the system contains local distortion or local disordering, we should start with the general expression (2). For a **mono-atomic** system (2) can be written in a simple form as follows;

$$S(Q,E) = A \left[1 + \frac{1}{N} \sum_{j \neq i} \langle \eta_i \eta_{i'} \rangle \exp(iQ \cdot [i' - i]) \delta(E - \hbar\omega_j) \right] \langle Q \rangle \quad (6)$$

where $A = \frac{1}{3N} \frac{\hbar^2 Q^2}{2M} e^{-2W} \frac{\langle n(E) + 1 \rangle}{E}$ and $\eta_j = \sqrt{3}(\mathbf{Q} \cdot \mathbf{e}^j)$ is the directional cosine of the displacement vector of the i^{th} atom to the scattering vector \mathbf{Q} . $\langle Q \rangle$ indicates an average over all directions of \mathbf{Q} .

Therefore, in summary, the double differential cross-section is

$$\frac{d^2\sigma}{d\Omega dE} = N \frac{k_1}{k_0} \langle b^2 \rangle S(Q,E) = N \frac{k_1}{k_0} \langle b^2 \rangle [S_s(Q,E) + S_d(Q,E)] \quad (7)$$

$$S(Q,E) = A [1 + S_d(Q,E)/A] \quad (8)$$

where $S(Q,E)$, $S_d(Q,E)$ and $S_s(Q,E)$ are the total, distinct and self scattering functions respectively. On the other hand in a total diffraction experiment the measured quantity is the static structure factor $S(Q) = \int S(Q,E) dE$ in the static approximation regime, i.e. $k_0 = k_1$,

$$\frac{d\sigma}{d\Omega} = N \langle b^2 \rangle S(Q) = N \langle b^2 \rangle [S_s(Q) + S_d(Q)] \quad (9)$$

$$S(Q) = 1 + S_d(Q) = \left[1 + \frac{1}{N} \sum_{i \neq i'} \exp(iQ \cdot [i' - i]) \right] \langle Q \rangle \quad (10)$$

This is related to a static pair correlation function $D_s(r)$ by

$$D_s(r) = (2/\pi) \int_0^\infty Q (S(Q) - 1) \sin(rQ) dQ \quad (11)$$

where the subtraction of unity from $S(Q)$ serves to remove the self scattering contribution. From the obvious similarity between (8) and (10) and analogy with (11) a dynamic pair correlation function (DPCF) is then defined as

$$D_d(r,E) = (2/\pi) \int_0^\infty Q \{ S(Q,E) / A - 1 \} \sin(rQ) dQ \quad (12)$$

$D_s(r)$ is essentially a density-density correlation function $\langle \rho(0)\rho(r) \rangle$ (where $\rho(r)$ is the density at r away from an origin atom), weighted according to the neutron scattering lengths at the origin and at r . $D_d(r,E)$ is also a density-density correlation function but with an additional weighting factor, which is $\langle \eta(0)\eta(r) \rangle$, i.e. the correlation between the directional cosine of $\mathbf{e}(r)$ at the energy E to the scattering vector \mathbf{Q} .

Since both correlation functions involve a density-density term, it is to be expected that $D_d(r,E)$ will exhibit features at the same distances as $D_s(r)$, but that the features will be weighted differently according to the atomic displacements of the relevant atoms for modes at energy E . Here, we should also stress that in the DPCF the contribution from light atoms is enhanced due to the mass-dependence of the cross-section.

APPLICATIONS

1) Vitreous SiO₂

The generalized phonon density of states (PDOS) measured on MARI for vitreous SiO₂ by application of the incoherent approximation shows a shoulder at 10meV and clear peaks at 50,100,133 and 150meV, shown in Fig.3. The dynamic pair correlation function $D_d(r,E)$ at a particular energy E , shown to be of interest by the PDOS, was calculated from the data in the following way. The $S(Q,E)$ at constant E was fitted by the expression

$$S_{fit}(Q,E) = C + A = C + B Q^2 \exp(-Q^2 \langle u^2 \rangle / 3) \quad (13)$$

The constant C represents the multiple scattering contribution to $S(Q,E)$ which is assumed to be independent of Q . The second term in (13) represents the self scattering A in (8) and the oscillation about the self scattering should be the distinct scattering. The fitted function was subtracted from the data and the result divided by the fitted self scattering to yield the integrand for the Fourier transform of (12).

Figure 4 shows the energy integrated $S(Q)$ of SiO₂ calculated from $S(Q,E)$ together with the Q -dependence of $S(Q,E)$ for energy transfers E of 12.5meV and 47.5meV. The 12.5meV data show a very similar form to $S(Q)$ with the exception that the first sharp diffraction peak which occurs at approximately 1.5\AA^{-1} in $S(Q)$ is absent from the inelastic data. Contrastingly, the 47.5meV data show an oscillatory behaviour which is essentially out of phase with $S(Q)$.

Figure 5 shows the static correlation function $D_s(r)$ according to (11) together with the dynamic correlation function $D_d(r,E)$ at 12.5meV and 47.5meV. The peaks in $D_s(r)$ may be identified as follows: 1.6\AA - Si-O bond; 2.6\AA - O-O distance in a tetrahedron; 3.1\AA - Si-Si distance between two Si in two corner-sharing tetrahedra; 4.0\AA - Si-O distance between atoms in different but connected tetrahedra, and 4.9\AA - both O-O distance between atoms in different but connected tetrahedra and Si to second Si distance.

A comparison of the $D_d(r,E=12.5\text{meV})$ with $D_s(r)$ shows a similarity in peak positions with different relative amplitudes, as expected. The first and second Si-O peaks are depressed relative to the first and second O-O peaks, indicating that the modes at this energy involve a relatively small amount of silicon motion compared to that of oxygen.

$D_d(r,E=47.5\text{meV})$ also exhibits peaks at the distances of the first two Si-O peaks in

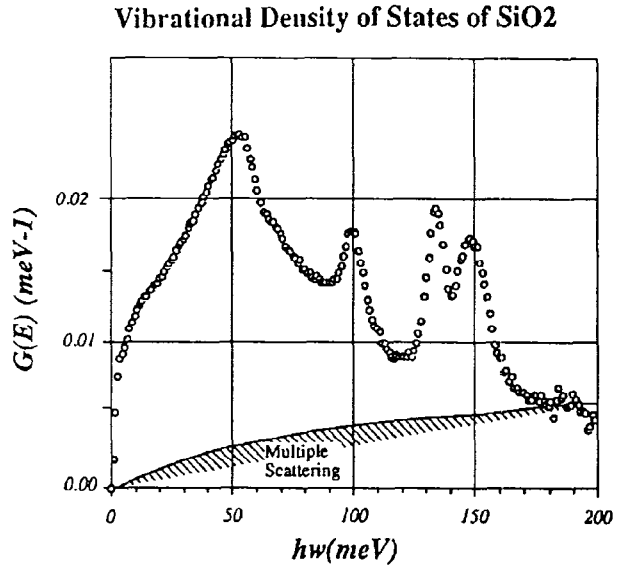


Fig.3 PDOS of g-SiO₂, $E_i=220\text{meV}$.

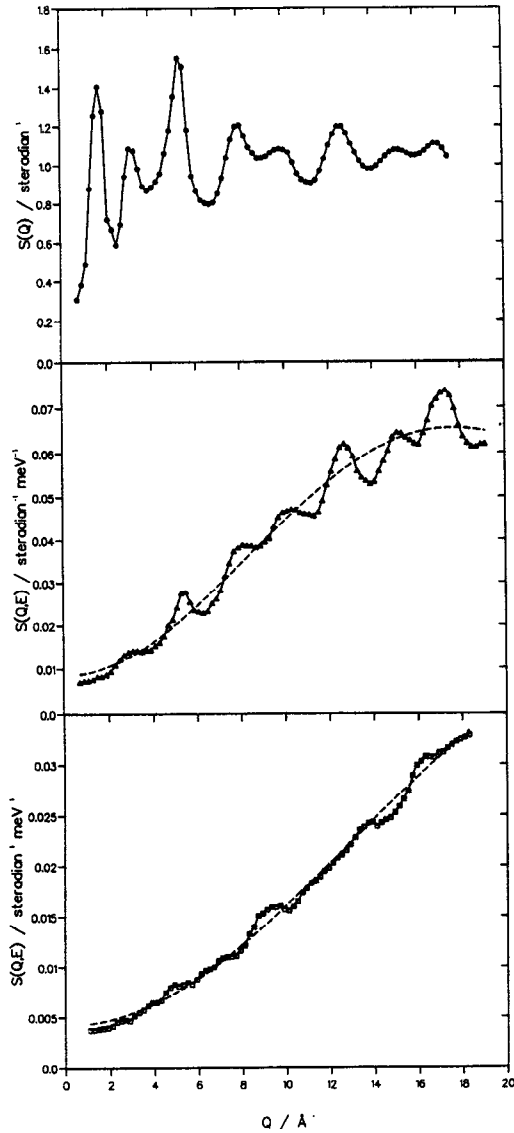


Fig.4 (a) $S(Q)$, (b) $S(Q,E=12.5\text{meV})$ and (c) $S(Q,E=47.5\text{meV})$. The dashed lines indicate the fit described in the text.

the weighting factor $\langle \eta(0)\eta(r) \rangle$ and other work has indicated that modes at this energy involve oxygens in a tetrahedron moving in directions which tend to oppose each other. From the results presented here it is clear that it is feasible to use a Fourier transform approach to extract information about atomic displacements in various modes from a measurement of the scattering function of a glass.

2) High- T_c oxide superconductors

Here we apply the DPCF method to the high- T_c superconductor $\text{YBa}_2\text{Cu}_3\text{O}_7$, which has very different masses for the constituent elements. In Table I we summarize the masses and the scattering cross-sections for $\text{YBa}_2\text{Cu}_3\text{O}_7$. The structure of this material has been studied by the diffraction technique and the *time averaged static structure* is well established

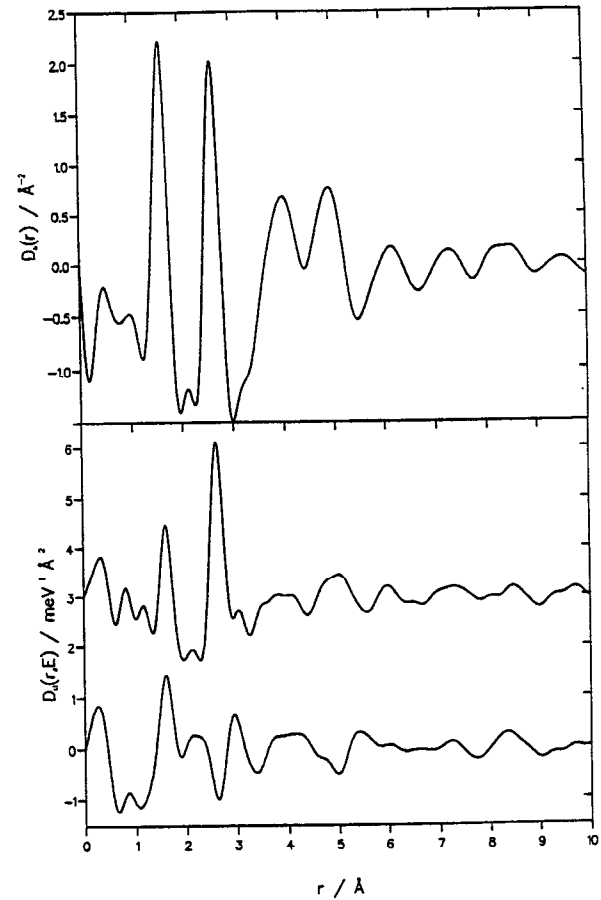


Fig.5 (a) $D_S(r)$, (b) $D_d(r,E=12.5\text{meV})$ and (c) $D_d(r,E=47.5\text{meV})$

$D_S(r)$. However, at the distances corresponding to both the first and second O-O peaks in $D_S(r)$ it is found that $D_d(r,E)$ has a negative-going peak.

This may be explained by a negative value from

the weighting factor $\langle \eta(0)\eta(r) \rangle$ and other work has indicated that modes at this energy involve oxygens in a tetrahedron moving in directions which tend to oppose each other.

From the results presented here it is clear that it is feasible to use a Fourier transform approach to extract information about atomic displacements in various modes from a measurement of the scattering function of a glass.

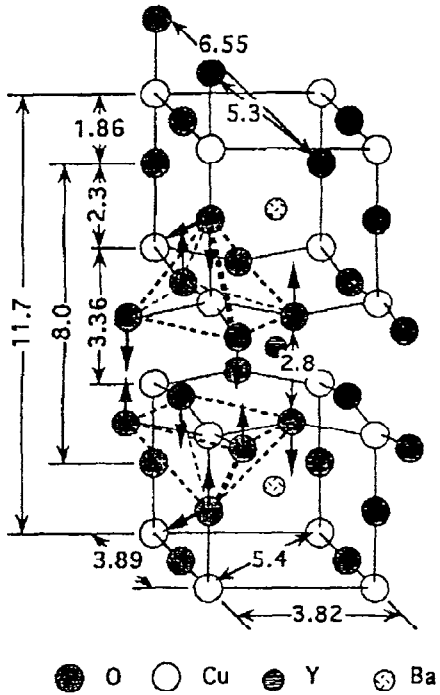


Fig.6 Crystal Structure of $\text{YBa}_2\text{Cu}_3\text{O}_7$.

by Rietveld refinement by assuming a crystal

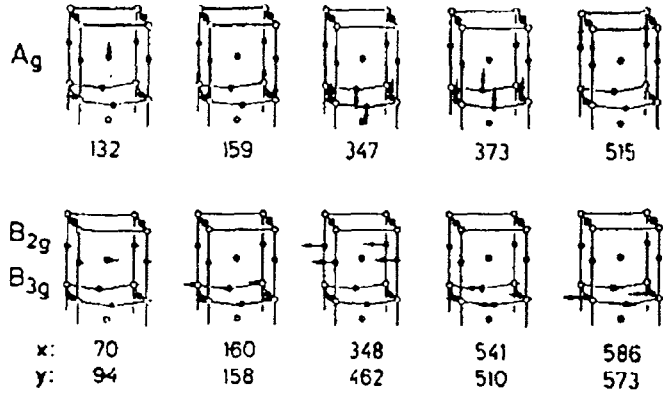


Fig.7 The 10 Raman-active vibrational modes out of 36 optical modes of $\text{YBa}_2\text{Cu}_3\text{O}_7$, taken from [6].

symmetry [5] as shown in Fig.6. From the structure symmetry group theory predicts 36 optical vibrational modes as depicted in Fig.7 [6]. Here we should note that oxygen modes dominate in the high frequency region, say above 40meV (320cm^{-1}). These modes have correlations dynamically only among the in-plane oxygens or among the apical oxygens, and there is no cross-correlations between these two types of modes.

The diffraction pattern will be dominated by contributions from atoms other than oxygen because of their relatively high scattering lengths. On the other hand for $S(Q,E)$ in the high energy region the dominating contribution is from the O-O correlations. The latter enhancement is due to two reasons: firstly the lighter mass of oxygen, cf. (5), secondly dominant oxygen modes in the high energy region, say above 40meV , as discussed in the previous paragraph. Therefore we can expect the $D_d(r,E)$ obtained from $S(Q,E)$ in the high energy region should have very different features from the $D_s(r)$ obtained from the diffraction pattern.

In Fig.8 the phonon density of states (PDOS) of $\text{YBa}_2\text{Cu}_3\text{O}_7$ is depicted and the dispersion relation is shown in Fig.9 [7]. The PDOS is composed of two types of features, i.e. sharp peaks and a broad feature under the peaks. The former are attributed to the flat

elements	A(amu)	$4\pi b^2$ (barns)
Y	89	7.8
Ba	137	3.5
Cu	64	7.4
O	16	4.2

Table I Atomic mass and scattering cross section for the elements of $\text{YBa}_2\text{Cu}_3\text{O}_7$.

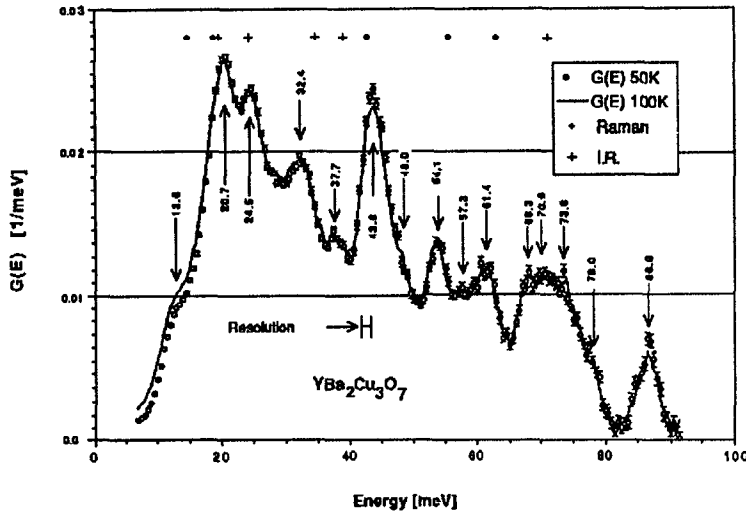


Fig.8 PDOS of $\text{YBa}_2\text{Cu}_3\text{O}_7$, $E_i=130\text{meV}$.

dispersion in the c -direction and the latter is attributed to the dispersive features in the a - b plane. In order to obtain meaningful results by use of the DPCF, we should take some energy band, $E_0 \pm \Delta E$, which completely contains the phonon dispersion curves of interest. For the first trial, the low energy limit was chosen at 40meV , where there is a gap in the PDOS and the dispersion relations. Therefore, by using the same method as described for g-SiO_2 in the previous section, $D_d(r, E)$ was obtained from $S(Q, E_0 \pm \Delta E)$, where $E_0 \pm \Delta E$ is from 40 to 90meV , whilst $D_s(r)$ was obtained from $S(Q)$, evaluated by integrating $S(Q, E)$ between -150 and 150meV . In Fig.10 $D_s(r)$ and $D_d(r, E)$ are superimposed. Obviously there are very large differences between them, and these differences are expected.

Because of the finite Q -range of the instrument the resolution in r -space does not

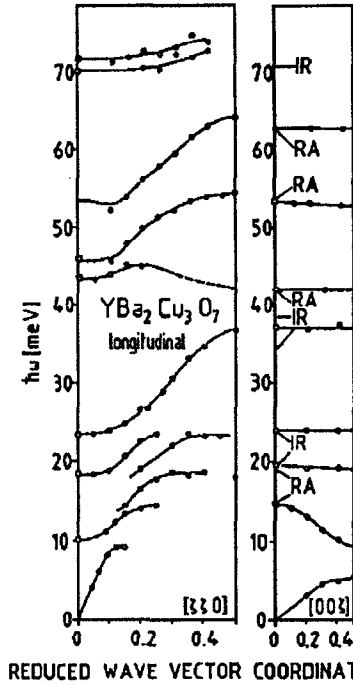


Fig.9 Phonon dispersion curve taken from [7].

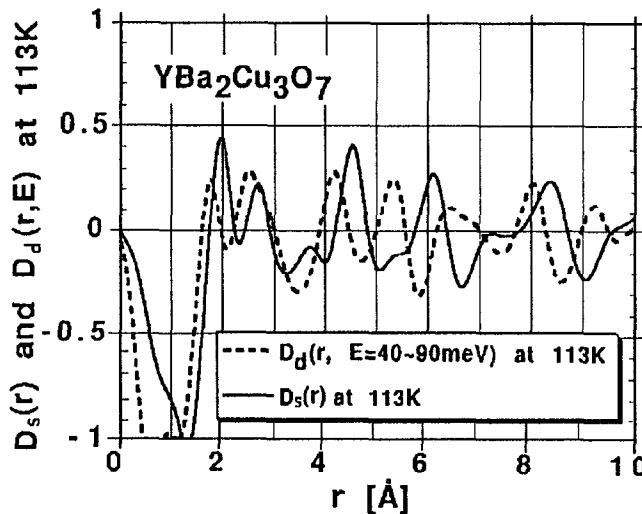


Fig.10 $D_s(r)$ and $D_d(r, E=40 \sim 90\text{meV})$ of $\text{YBa}_2\text{Cu}_3\text{O}_7$.

resolve all details. However, $D_S(r)$ has a similar behaviour to that observed by the use of the LAD diffractometer [8]. On the other hand it is found that the peaks in $D_d(r,E)$ at 1.8, 2.4, 4.2, 5.4, 6.5 and 8.0 Å correspond to the atomic distances between oxygens as shown in Fig. 6. We should note that those correlations are among the oxygens in a group which participate to a certain mode, there is no cross-correlations between the different groups of oxygens because of the orthogonalization, for instance between the in-plane oxygens and the apical oxygens. Thus we may conclude that the DPCF method provides the specific correlations between specific atoms in the material without isotope substitution!! (ie. a Dynamical Labelling Method) Although a quantitative understanding of the intensity of $D_d(r,E)$ has not yet been performed, we have, however, demonstrated that the DPCF provides a promising new approach to the structural study of materials. In particular the DPCF method may be applied to study local structural distortion, which may be one of the most important properties relating to high- T_C superconductivity [9,10].

FURTHER SUGGESTIONS

We may also suggest that the dynamic pair correlation function $D_d(r,E)$ contains information on the dynamically moving structure, as the name says. If the movement of the atoms is much slower than the neutron speed, $D_d(r,E)$ may show the instantaneous position of atoms. For instance, if an atom has an anharmonic oscillation in a double well potential, $D_d(r,E)$ may resolve the local stable positions, whereas the diffraction refinement may show just the time-averaged single position associated with a broad thermal diffuse factor. This argument is the direct result of the standard neutron scattering cross-section, but it has not been clearly proved so far.

REFERENCES

- [1] J.M.Carpenter and C.A.Pelizzari, Phys. Rev. B **12**, 2397 (1975)
- [2] M.Arai, A.D.Taylor, S.M.Bennington and Z.A.Bowden, Recent Developments in the Physics of Fluids, Adam Hilger, F321 (1991)
- [3] M.Arai, A.C.Hannon, A.D.Taylor, A.C.Wright, R.N.Sinclair and D.L.Price, Trans. ACA **27**(1991)113.
A.C.Hannon, M.Arai, R.N.Sinclair and A.C.Wright, J. Non-Cryst. Solids **150**, 239 (1992).
- [4] Methods of Experimental Physics Vol.23, p.26, eds. K.Sköld and D.L.Price, Academic Press 1986
- [5] J.D.Jorgensen, B.W.Veal, A.P.Paulikas, L.J.Nowicki, G.W.Crabtree, H.Claus and W.K.Kwok, Phys. Rev. B **41**, 1863 (1990)
- [6] R.Liu, C.Thomsen, W.Kress, M.Cardona, B.Gegenheimer, F.W. de Wette, J.Prade, A.D.Kulkarni and U.Schröder, Phys. Rev. B **37**, 7971 (1988)
- [7] W.Reichardt, Physica C **162-164**, 464 (1989)
- [8] R.L.McGreevy, L.Borjesson, L.M.Torell and W.S.Howells, Physica **B180-181**, 443 (1992)
- [9] T.Egami and S.J.L.Billinge, in: Proc. of The Fifth International Symposium on Superconductivity, Nov. 16-19, 1992 Kobe, Japan, Springer-Verlag.